Video Article

Cellular Redox Profiling Using High-content Microscopy

Tom Sieprath[1,2], Tobias Corne[1,2], Joke Robijns[1], Werner J. H. Koopman[3], Winnok H. De Vos[1,2]

[1]Laboratory of Cell Biology and Histology, Department of Veterinary Sciences, University of Antwerp

[2]Cell Systems and Imaging Research Group (CSI), Department of Molecular Biotechnology, Ghent University

[3]Department of Biochemistry , Radboud Institute for Molecular Life Sciences, Radboud University Medical Center

Correspondence to: Winnok H. De Vos at winnok.devos@uantwerpen.be

URL: https://www.jove.com/video/55449
DOI: doi:10.3791/55449

Keywords: Cellular Biology, Issue 123, Reactive Oxygen Species, Mitochondria, Mitochondrial Morphofunction, Live Cell Imaging, High-content Microscopy, Fluorescence Microscopy, Quantitative Multiparametric Microscopy, Redox Biology

Date Published: 5/14/2017

Citation: Sieprath, T., Corne, T., Robijns, J., Koopman, W.J., De Vos, W.H. Cellular Redox Profiling Using High-content Microscopy. *J. Vis. Exp.* (123), e55449, doi:10.3791/55449 (2017).

Abstract

Reactive oxygen species (ROS) regulate essential cellular processes including gene expression, migration, differentiation and proliferation. However, excessive ROS levels induce a state of oxidative stress, which is accompanied by irreversible oxidative damage to DNA, lipids and proteins. Thus, quantification of ROS provides a direct proxy for cellular health condition. Since mitochondria are among the major cellular sources and targets of ROS, joint analysis of mitochondrial function and ROS production in the same cells is crucial for better understanding the interconnection in pathophysiological conditions. Therefore, a high-content microscopy-based strategy was developed for simultaneous quantification of intracellular ROS levels, mitochondrial membrane potential ($\Delta\Psi_m$) and mitochondrial morphology. It is based on automated widefield fluorescence microscopy and image analysis of living adherent cells, grown in multi-well plates, and stained with the cell-permeable fluorescent reporter molecules CM-H_2DCFDA (ROS) and TMRM ($\Delta\Psi_m$ and mitochondrial morphology). In contrast with fluorimetry or flow-cytometry, this strategy allows quantification of subcellular parameters at the level of the individual cell with high spatiotemporal resolution, both before and after experimental stimulation. Importantly, the image-based nature of the method allows extracting morphological parameters in addition to signal intensities. The combined feature set is used for explorative and statistical multivariate data analysis to detect differences between subpopulations, cell types and/or treatments. Here, a detailed description of the assay is provided, along with an example experiment that proves its potential for unambiguous discrimination between cellular states after chemical perturbation.

Video Link

The video component of this article can be found at https://www.jove.com/video/55449/

Introduction

The concentration of intracellular ROS is meticulously regulated through a dynamic interplay between ROS producing and ROS defusing systems. Imbalance between the two provokes a state of oxidative stress. Among the major sources of ROS are mitochondria[1]. Given their role in cellular respiration, they are responsible for the bulk of intracellular superoxide ($O_2^{\bullet-}$) molecules[2]. This mostly results from electron leakage to O_2 at complex 1 of the electron transport chain under conditions of strong negative inner mitochondrial membrane potential ($\Delta\psi_m$), *i.e.*, mitochondrial hyperpolarization. On the other hand, mitochondrial depolarization has also been correlated with increased ROS production pointing to multiple modes of action[3,4,5,6,7,8]. Furthermore, through redox modifications in proteins of the fission-fusion machinery, ROS co-regulate mitochondrial morphology[9].For example, fragmentation is correlated with increased ROS production and apoptosis[10,11], while filamentous mitochondria have been linked to nutrient starvation and protection against mitophagy[12]. Given the intricate relationship between cellular ROS and mitochondrial morphofunction, both should ideally be quantified simultaneously in living cells. To do exactly this, a high-content imaging assay was developed based on automated widefield microscopy and image analysis of adherent cell cultures stained with the fluorescent probes CM-H_2DCFDA (ROS) and TMRM (mitochondrial $\Delta\psi_m$ and morphology). High-content imaging refers to the extraction of spatiotemporally rich (*i.e.*, large number of descriptive features) information about cellular phenotypes using multiple complementary markers and automated image analyses. When combined with automated microscopy many samples can be screened in parallel (*i.e.* high-throughput), thereby increasing the statistical power of the assay. Indeed, a main asset of the protocol is that it allows for simultaneous quantification of multiple parameters in the same cell, and this for a large number of cells and conditions.

The protocol is divided into 8 parts (described in detail in the protocol below): 1) Seeding cells in a 96-well plate; 2) Preparation of stock solutions, working solutions and imaging buffer; 3) Setting up of the microscope; 4) Loading of the cells with CM-H_2DCFDA and TMRM; 5) First live imaging round to measure basal ROS levels and mitochondrial morphofunction; 6) Second live imaging round after addition of *tert*-butyl peroxide (TBHP) to measure induced ROS levels; 7) Automated image analysis; 8) Data Analysis, Quality Control and Visualization.

The assay was originally developed for normal human dermal fibroblasts (NHDF). Since these cells are large and flat, they are well suited for assessing mitochondrial morphology in 2D widefield images[13,14]. However, with minor modifications, this method is applicable to other adherent

cell types. Moreover, next to the combination of CM-H_2DCFDA and TMRM, the workflow complies with a variety of fluorescent dye pairs with different molecular specificities[1,15].

Protocol

The protocol below is described as performed for NHDF cells and with use of the multiwell plates specified in the materials file. See **Figure 1** for a general overview of the workflow.

1. Preparation of Reagents

1. Prepare complete medium by supplementing Dulbecco's Modified Eagle Medium (DMEM) with 10% v/v Fetal Bovine Serum (FBS) and 100 IU/mL penicillin and 100 IU/mL streptomycin (PS). For 500 mL complete medium, add 50 mL of FBS and 5 mL of PS to 445 mL of DMEM.
2. Prepare HBSS-HEPES (HH) imaging buffer by supplementing Hank's Balanced Salt Solution (with magnesium and calcium, but without phenol red) with 20 mM HEPES. For 500 mL HH, add 10 mL of 1M HEPES stock solution to 490 mL HBSS. Verify the pH and, if necessary, adjust to pH 7.2.
3. **Prepare 1 mM CM-H_2DCFDA stock solution by dissolving 50 µg of CM-H_2DCFDA lyophilized powder in 86.5 µL anhydrous DMSO. Mix by vortexing or pipetting up and down and make 20 µL aliquots in brown microcentrifuge tubes. Store in the dark at -20 °C and use within 1 week. If stored under N_2-atmosphere shelf life can be increased up to at least 1 month.**
    1. Prepare 1 mM TMRM stock solution by dissolving 25 mg TMRM powder in 50 mL anhydrous DMSO. Mix by vortexing or pipetting up and down and make 10 µL aliquots in brown microcentrifuge tubes. Store in the dark at -20 °C. This solution is stable for at least a year.
4. Prepare a fresh aliquot of *Tert*-butyl peroxide (TBHP) stock (~ 7 M) for every experiment by directly pipetting a volume from the 70% stock solution (10 µL/96-well plate). Keep this aliquot at 4 °C until further use.
5. Prepare antibody working solution (AB) by diluting two secondary antibodies (Alexa Fluor 488 donkey anti-rabbit and CY3 donkey anti-rabbit) 1,000 times in 1x HH-buffer.

2. Setting Up of the Microscope and Acquisition Protocol (± 15 min)

NOTE: Image acquisition is performed with a wide-field microscope equipped with an automated stage and shutters, and a hardware based autofocus system using a 20X air Plan-corrected objective (NA = 0.75) and an EM-CCD camera. When setting up the assay for the first time, a test plate containing control cells, stained according to the protocol's instructions is used to calibrate the XY-stage and to optimize the acquisition settings. If the acquisition settings have already been determined, calibration can be done using an empty plate.

1. Lower the objective to the absolute base level and calibrate the XY-stage following software instructions.
2. Make sure the correct filter cubes are installed. To visualize CM-H_2DCFDA, use a standard GFP filter cube with a 472/30 nm excitation bandpass filter, a 495 nm cutoff dichroic mirror and a 520/35 nm bandpass emission filter. For TMRM, use a filter cube for TRITC with a 540/25 nm bandpass excitation filter, a 565 nm cutoff dichroic mirror and a 605/55 nm bandpass emission filter.
3. **Create an imaging protocol using the acquisition software.**
    1. Select the correct type of multiwell plate (manufacturer and code) from the list of available plates provided within the software. Alternatively define your own multiwell plate format using plate and well dimensions.
    2. Align the well plate according to the software's instructions, *e.g.* by defining two corners of the four outer corner wells. This step covers for camera orientation variation.
    3. Select the wells that need to be acquired. If this option is not available in the software, use a set of manually defined XY-locations that correspond to the selected wells.
    4. Optimize the acquisition settings (exposure time, lamp intensity, EM-gain) for the two channels separately using the test plate. Minimize exposure and intensity as fluorescence excitation light itself induces ROS. But, make sure the signal to background ratio is at least 2 for basal CM-H_2DCFDA and 3 for TMRM before TBHP treatment, and that there is no saturation after TBHP treatment. Acquisition settings greatly depend on the microscopy setup and cell type used, but as a reference, indicative settings when using a metal halide light bulb of 130 W as light source and NHDF cells stained according to the protocol's instructions are the following: for both CM-H_2DCFDA and TMRM an exposure time of 200 ms and ND filter 8 are used, combined with an EM-gain of 15 (13 MHz; 14-bit) and 4 (27 MHz; 14-bit) respectively. Once optimized for a certain setup and cell type, this step can be skipped.
    NOTE: it is essential that acquisition settings be kept the same throughout the entire imaging process. For large-scale, multi-day experiments, lamp stability should be warranted by regular quality control.
    5. Define an acquisition protocol, consisting of a sequential lambda (wavelength) acquisition. Select the CM-H_2DCFDA channel to be acquired first, to minimize light exposure before the measurement.
    6. Define a well-plate loop, to acquire 4 regularly spaced non-overlapping images positioned around the center of each well of the well selection using the acquisition protocol defined in 2.3.4. Choose meandering image acquisition, *i.e.,* first from left to right, from well B02 to B11, then back, from right to left, from well C11 to C02 and so on (**Figure 2A**). This saves time compared to left-to-right image acquisition. If this option is not available in the software, adjust the custom set of XY-locations created in 2.3.3 to take on this imaging pattern.
    7. Save the XY-coordinates of the imaging-positions (*e.g.* in a separate xml-file), to allow easy revisiting in case of microscope recalibration. This is especially important if the readout from this assay has to be correlated with a post-hoc immunofluorescence (IF) staining for the same cells.

3. Seeding Cells in a 96-well Plate (45 - 90 min, Depending on the Number of Different Cell Lines)

1. Work in sterile environment such as a class 2 biosafety cabinet and wear gloves.
2. Decontaminate all surfaces and materials using 70% v/v ethanol in distilled water.
3. Take a cell culture flask with a 90% confluent cell culture from the incubator and place it in the biosafety cabinet.
4. Wash the cells twice with PBS 1x.
5. Add the appropriate amount of 0.05% trypsin-EDTA solution on the cells, making sure that the complete cell surface is covered (*e.g.*, 1 mL for a T25 flask), and incubate for 2 min at 37 °C and 5% CO_2.
6. If all cells are detached (check with a microscope), add culture medium (DMEM + 10% FBS + 1% penicillin-streptomycin; ± 4 mL in a T25 flask) to inactivate the trypsin-EDTA solution.
7. Centrifuge for 5 min at 300 x g at room temperature.
8. Discard the supernatant and resuspend the cell pellet in culture medium. Determine the amount of medium for every cell type to obtain a cell concentration that is compatible with cell counting. Typically, a 90% confluent T25 flask of NHDF contains about 1-1.5 million cells, which are resuspended in 3-4 mL of culture medium.
9. Count the cells using a cell counting chamber or Coulter counter.
10. Seed 8,000-10,000 cells in each of the inner 60 wells of a black 96-well plate with a thin continuous polystyrene or glass bottom (black to avoid scattering and cross-talk between adjacent wells during imaging). When using different conditions/treatments/cell lines, distribute their seeding locations homogeneously on the plate so as to minimize plate effects (**Figure 2A**). The outer wells, except for well B01 and A01, are not used because they are more prone to edge effects.
11. Seed 8,000-10,000 cells in B01. This well will be used for focus adjustment, just prior to the image acquisition.
12. Fill the empty outer wells with medium to minimize gradients (temperature, humidity, *etc.*) between the wells and the environment.
13. Gently tap the plate three times before placing it back into the incubator to avoid cells from growing in patches.
14. Culture the cells for 24 h, or up to a confluence degree of approx. 70%.
15. Save the treatment information for the experiment into a spreadsheet called "Setup.xlsx". The file should contain four columns and will be used to link treatments with wells and image information during data analysis. The four columns are: 'Well', 'Treatmentnumber', 'Treatment' and 'Control' (one row per well). Every treatment is coupled with a unique treatment number, which is used during data visualization to determine the order of the treatments on the X-axis of plots. The control-column specifies the treatment that functions as control for the treatment on the current row. Illustrations of a typical experimental layout and corresponding setup file are depicted in **Figure 2**.

4. Loading of the Cells with CM-H_2DCFDA and TMRM (± 45 min)

NOTE: Handling of the cells on the day of the experiment can be carried out in a sterile environment (biosafety cabinet), but this is not mandatory because cells will be discarded or fixed directly after the assay.

1. Heat the HH-buffer to 37 °C.
2. Prepare a 20 µM TMRM working solution by diluting the 1 mM stock solution 50 times in HH-buffer (add 490 µL of HH-buffer to 1 aliquot of 10 µL TMRM stock solution).
3. **Prepare a loading solution with 2 µM CM-H_2DCFDA and 100 nM TMRM. To this end, dilute the 1 mM CM-H_2DCFDA stock solution 500x and the 20 µM TMRM working solution 200x in HH-buffer.**
    1. Typically, for 60 wells, prepare 7.5 mL of loading solution by adding 15 µL of CM-H_2DCFDA and 37.5 µL of TMRM solution to 7447.5 µL of HH.
4. Discard the culture medium from the cells by turning the plate upside down in a single fluid motion.
5. Gently wash the cells twice with HH-buffer using a multichannel pipette (100 µL/well). Discard the HH-buffer in between the washing steps by turning the plate upside down in a single fluid motion.
6. Load the cells with CM-H_2DCFDA and TMRM by adding 100 µL of the loading solution to each well, again using a multichannel pipette. Incubate for 25 min in the dark, at room temperature. Don't forget well B01.
7. **During these 25 min, prepare working solutions of the oxidant TBHP and make sure the microscope and accessory hardware are turned on.**
    1. Prepare working solution I: Dilute the 7M stock solution 70x to 100 mM (10 µL stock in 690 µL HH-buffer).
    2. Prepare working solution II: Dilute WS I 100x to 1 mM (10 µL WS I in 990 µL HH-buffer).
    3. Prepare working solution III: Dilute WS III 25x to 40 µM (for 60 wells add 300 µL WS II in 7200 µL HH buffer).
8. After 25 min, wash the cells again twice with 100 µL HH-buffer as described before.
9. Add 100 µL of HH-buffer to all 60 inner wells.

5. First Live Imaging Round to Measure Basal ROS Levels and Mitochondrial Morphofunction (± 15 min)

1. Make sure the acquisition software is operational and the imaging protocol is loaded.
2. Install the plate on the microscope, turn on the hardware based autofocus system and use well B01 to adjust the autofocus offset using the TMRM channel. As this procedure induces an increase in CM-H_2DCFDA signal intensity, this well is excluded from downstream image analysis.
3. Run the imaging protocol.

6. Second Live Imaging Round after Addition of TBHP to Measure Induced ROS Levels (± 20 min)

1. Carefully remove the 96-well plate from the microscope.
2. Add 100 µL of TBHP WS III (40 µM) to each well using a multichannel pipette (This results in a 20 µM TBHP concentration in the wells). This compound is used as an internal positive control for the CM-H_2DCFDA staining (the signal should rise) as well as a means to measure induced ROS levels.
   NOTE: H_2O_2 can also be used instead of TBHP, but this compound is less stable and therefore less reliable.
3. Wait at least 3 min to allow complete reaction of TBHP with CM-H_2DCFDA.
4. During this time, add 100 µL antibody working solution (1/1,000) to well A01.
5. Mount the plate back on the microscope and check focus again using well B01.
6. Acquire the same positions as in the first imaging round using the same imaging protocol.
7. Export the acquired datasets in a single folder as individual tiff files using standardized nomenclature that includes reference to the plate, pre- or post-TBHP treatment, well, field and channel, separated by underscores, *e.g.* 'P01_Pre_B02_0001_C1' for plate 1, pre-TBHP treatment, well B02, field 1 and channel 1. This information will be used during image analysis (*e.g.* to select the appropriate segmentation settings), as well as during data analysis (to connect analysis data with the correct treatments).
8. Acquire flat field images for both channels on all four positions around the center of well A01 using the acquisition protocol. Save them as individual tiff files in the same folder as the other images using the following standardized nomenclature: 'P01_FF_A01_0001_C1' for plate 1, field 1 and channel 1. Make sure the signals are well within the dynamic range; in case of saturation, use a lower concentration of antibody working solution.
9. Discard the plate or save for further processing.
   NOTE: Instead of removing the plate from the microscope and using a multichannel pipette to add the TBHP solution, an automated pipette can be installed on the microscope stage and connected with the acquisition software so as to function upon receiving a trigger. This allows for adding TBHP to every well directly after the first acquisition, before moving to the next well. This way, when the first imaging round is finished, the second one can start right away and all wells will have had an equal incubation time with the TBHP.

7. Image Processing and Analysis (± 30 min per 96-well plate)

NOTE: All image processing is performed in FIJI (http://fiji.sc), a packaged version of ImageJ freeware. A dedicated script was written for automated analysis of intracellular ROS- and mitochondrial signals, as well as morphological parameters (RedoxMetrics.ijm, available upon request). The underlying algorithms are described in Sieprath *et al.*[1].

1. Make sure FIJI is installed and operational.
2. Start up FIJI and install the macro-set (Plugins - > Macros - > Install …). This will invoke a number of new macro commands as well as a set of action tools to optimize the analysis settings, as shown in **Figure 3A**.
3. **Open the setup interface to set the analysis settings by clicking on the 'S' button (Figure 3B).**
   1. Select the image type, the number of channels and the well that was used for acquiring flatfield images.
   2. Indicate which channel contains cells (CM-H_2DCFDA channel) or mitochondria (TMRM-channel) and adjust the pre-processing and segmentation parameters for each channel depending on the image quality (**Figure 3B**). Tick the 'Background' and 'Contrast' checkboxes to perform background subtraction or contrast limited adaptive histogram equalization[16], respectively. Define a sigma for Gaussian blurring of cells and Laplacian enhancement of mitochondria. Select an automatic thresholding algorithm and fill in the size exclusion limits (in pixels). If a fixed threshold is chosen instead of an automatic thresholding algorithm, fill in the upper threshold.
   3. Test the segmentation settings on a few selected images of the acquired data sets by opening them and clicking the 'C' or 'M' buttons in the menu for cell- or mitochondria segmentation respectively, and adjust the settings if necessary. An example result is shown in **Figure 3C**.
4. Run the batch analysis on the folder(s) of interest by clicking on the '#' button and selecting the folder with the images. Per folder, this will produce a new 'Output' directory, containing individual ROI sets (zip files) and result files (.txt) per image. For both channels the results file contains intensity and morphological descriptors. The CM-H_2DCFDA channel (cells) results file contains per descriptor the average value for the combined ROIs within one image. For the TMRM channel, the results file contains per descriptor the value for every individually segmented mitochondrial ROI.
5. After batch analysis, visually verify the segmentation performance on a 'Verification stack', a hyperstack of all images with their respective ROI overlay by clicking on the 'V' button. This way, artifacts such as over-/undersegmentation, out of focus images or dust-particles/fibers in images can already be spotted quickly. Further curation can be done during data quality control (cfr. §8).

8. Data Analysis, Quality Control (QC) and Visualization

Processing and analysis of the raw data is done using R statistical freeware (http://www.rproject.org – version 3.3.2) and RStudio (http://www.rstudio.com/ – version 1.0.44). To quickly obtain and visualize the results, an intuitive Shiny application[17] (available upon request) has been conceived that integrates and visualizes the data in heatmaps and boxplots, and also performs statistical analyses. In general, the workflow comprises of two consecutive steps. First, data is processed and inspected per 96-well plate to detect aberrant data points. Secondly, curated data from all plates of a given experiment are combined and analyzed using non-parametric multivariate tests[18] and a principal component analysis.

1. Make sure R and RStudio are installed and operational.
2. Start RStudio.
3. Open the RedoxMetrics shiny application and run the app (choose to run it in an external browser).
4. On the 'input' page, select the directory where the results files from RedoxMetrics.ijm are located.

5. Make sure 'Setup.xlsx' (created in step 3.15) is also present inside this directory.
6. **The results files and setup information are automatically imported, rearranged and visualized.**
    1. The 'experimental setup' page shows the layout of the experiment. Use this page for verification.
    2. The next page, 'results per plate' shows the data for each plate separately in a color-coded multi-well plate layout as well as in boxplots with outliers labeled with well name and image number. The latter allows facile inspection and identification of aberrant data points (extremely high or low values compared to the average values measured for that specific treatment - see **Figure 4** for an example). Using this information, verify the images corresponding to the aberrant points. If abnormalities are detected, they have to be removed from the analysis. Most abnormalities are caused by improper segmentation when (part) of the image is out of focus, or when highly fluorescent dust particles disturb proper segmentation. Extreme cases can already be spotted quickly using the verification stack tool (step 7.5), but more subtle occurrences are discovered at this step. When no apparent or technical reason can be found for the aberrant value, the image should not be removed from analysis.
    3. Optional: create a new spreadsheet called 'Drop.xlsx' with only one column called 'Drop'. In this column, list the file names (including ".tif" extension) of all the images that have to be removed from the analysis (identified in step 7.5 or step 8.6.2). Upload this file using the 'input' page.
    4. The 'results whole experiment' page shows the results from all plates combined. If a drop file was uploaded, this file is used to remove the specified data points from the analysis.
    For each parameter individually, the data are normalized per plate according to their respective controls. Data from all plates are then combined, followed by non-parametric multivariate tests from the nparcomp package[18]. If only 2 treatments are compared two sample tests for the nonparametric Behrens-Fisher problem are performed. For more than 2 treatments, a non-parametric contrast-based multiple comparison test is used. The results are visualized using boxplots.
    5. The 'cluster analysis' page shows the results of a principal component analysis (PCA - R core 'stats' package). Data from 5 parameters (basal & induced ROS, and mitochondrial membrane potential, size & circularity) are combined to discriminate the different treatments based on a sensitive redox profile. To this end, a principal component analysis (PCA) is performed (R core 'stats' package). The results are visualized using a biplot (ggbiplot package - http://github.com/vqv/ggbiplot).
    6. Use the 'download data' page to download the backend data frames containing the processed and rearranged data such that they can be reused for more advanced data visualization or statistical analyses.
    NOTE: Typical pitfalls and potential solutions are listed in **Table 1**.

Representative Results

The assay has been benchmarked using several control experiments, the results of which are described in Sieprath *et al.*[1]. In brief, the fluorescence response of CM-H_2DCFDA and TMRM to extraneously induced changes in intracellular ROS and $\Delta\psi_m$, respectively has been quantified to determine the dynamic range. For CM-H_2DCFDA, NHDF showed a linear increase in fluorescence signal when treated with increasing concentrations of TBHP between a range of 10 µM to 160 µM. Likewise, for TMRM, NHDF cells demonstrated a linear increase in mitochondrial fluorescence when treated with increasing concentrations of oligomycin (which induces $\Delta\psi_m$ hyperpolarization) within a 1 to 10 µg/µL range. Conversely, real-time addition of valinomycin, an antibiotic that induces $\Delta\psi_m$ depolarization, resulted in a gradual, quantifiable decrease of TMRM fluorescence.

The assay has also been used in a variety of experiments to reveal differences in redox status between cell types or treatments[1,15]. To illustrate this, the results are shown of an experiment in which NHDF were treated with the HIV protease inhibitor Saquinavir (SQV) (**Figure 5**). Using the described protocol, a significant increase was detected for both basal and induced ROS levels as compared to control cells treated with DMSO (**Figure 5B**). SQV treatment also significantly affected mitochondrial morphofunction. Morphologically, mitochondria acquired a highly fragmented pattern, which was also confirmed by a higher circularity and smaller average size of the individual mitochondria. Functionally, $\Delta\psi_m$, measured as average TMRM signal per mitochondrial pixel was also significantly increased (**Figure 5A**). When combining the data of the 5 parameters described above, the two conditions (control and SQV) could be clearly separated from each other by principal component analysis. Data from three independent biological replicates is shown in a 2D-biplot displaying the first two principal components, which explain 81.4% of the total variance (**Figure 5C**). This proves the robustness of the assay and suggests that the combined readout may serve as a sensitive indicator of cellular health status.

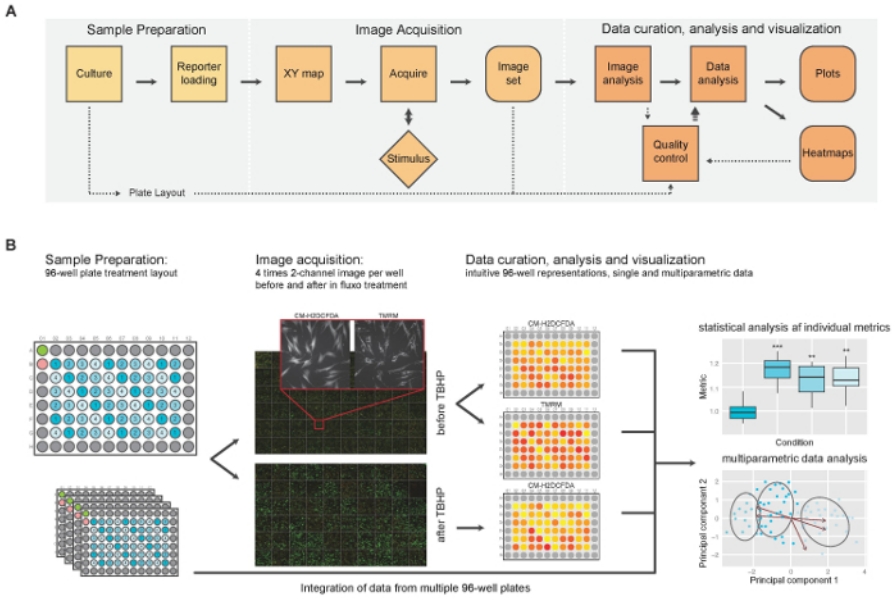

Figure 1: General Overview of the High-content Imaging Assay for Simultaneous Measurement of Intracellular Basal and Induced ROS Levels and Mitochondrial Morphofunction. (**A**) Schematic representation of the major operational blocks. (**B**) Illustrated example: cells are seeded in multiple identical 96-well plates. A standard well plate layout is shown in more detail in **Figure 2A**. After staining, 4 images are acquired per channel around the center of each well, both *pre* and *post TBHP* treatment, which is illustrated by the large montages with inset. After image analysis, intensity results are visualized using an intuitive heat-map projected onto the well-plate layout. This permits rapid detection of plate effects or aberrant wells. After curation of the complete experimental data sets, final data analysis is performed resulting in single- as well as multi-parameter output. (This figure was modified from reference[1], with permission of Springer) Please click here to view a larger version of this figure.

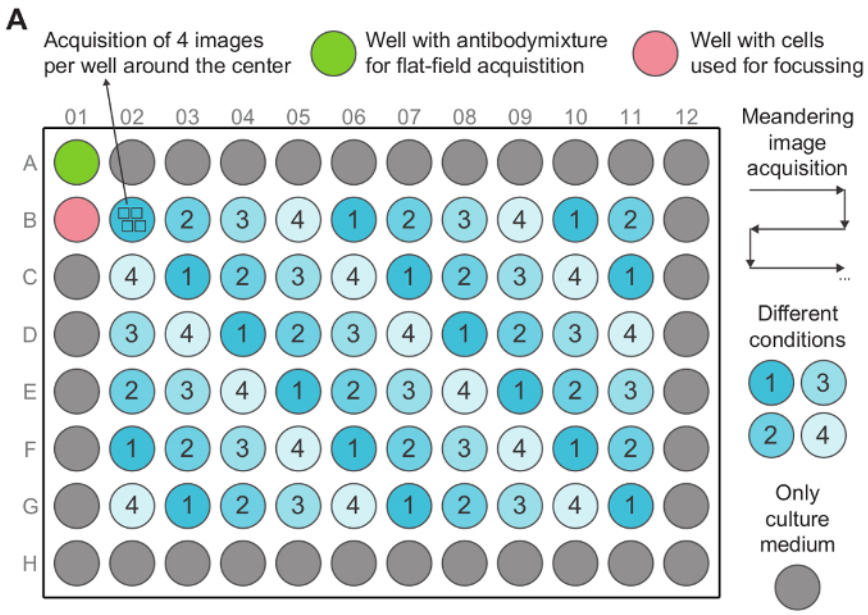

B Setup.xlsx

	A	B	C	D
1	Well	Treatmentnumber	Treatment	Control
2	B02	1	Treatment 1	Treatment 1
3	B03	2	Treatment 2	Treatment 1
4	B04	3	Treatment 3	Treatment 1
5	B05	4	Treatment 4	Treatment 1
6	B06	1	Treatment 1	Treatment 1

Figure 2: A Typical Experimental 96-well Layout and Corresponding 'Setup' File. (**A**) 4 different conditions are distributed homogeneously across the inner 60 wells of the plate. Well B01 also contains cells, but is only used to adjust the initial PFS offset just before imaging. The other outer wells are filled only with culture medium to minimize gradients (temperature, humidity, *etc.*) during cell culture. Image acquisition is performed in a meandering manner, *i.e.,* first from left to right, from well B02 to B11, then back, from right to left, from well C11 to C02 and so on. After image acquisition flat field images are acquired in well A01, which is used for correcting spatial illumination heterogeneity during image analysis. (**B**) The corresponding setup file (Setup.xlsx) is a spreadsheet that contains information about the layout of the experiment. It specifies the locations of each treatment in the multiwell plate and their respective controls. Each row represents a well. Each treatment has its own unique treatment number, which is used to specify the order of the treatments on the X-axis of the generated plots during data analysis. The 'Control' column contains the treatment that should be used as a control for normalizing the data of the treatment specified in the same row. In the example, treatment 1 is the treatment that is used as control for normalizing the data from all the other treatments. Please click here to view a larger version of this figure.

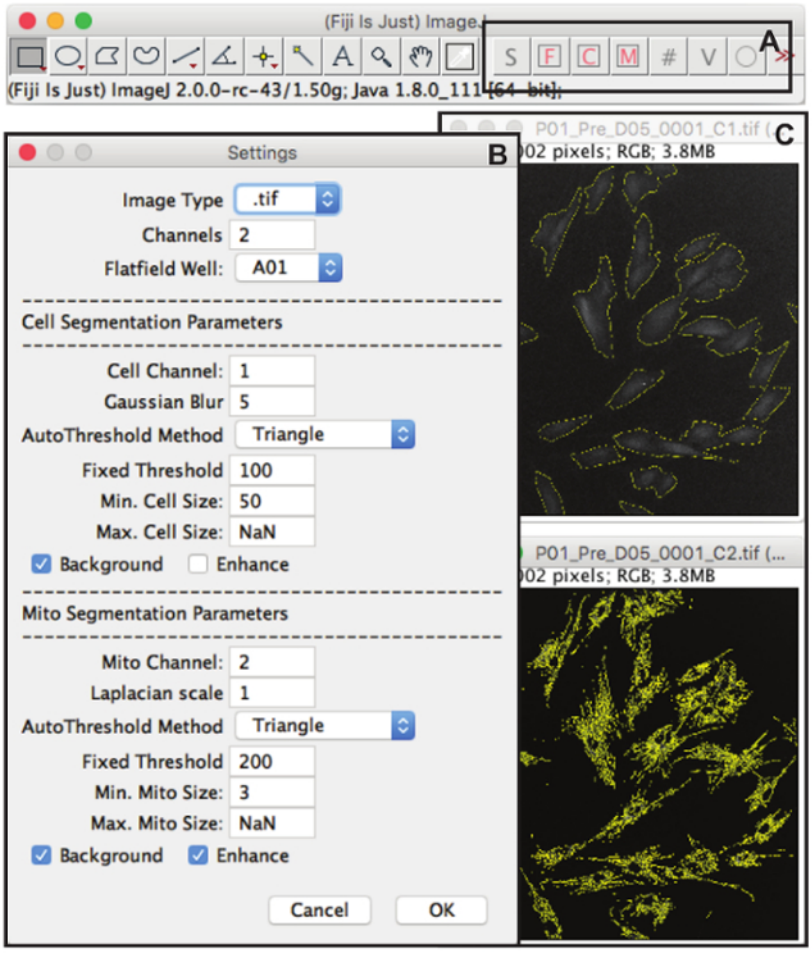

Figure 3: RedoxMetrics Macro-set, Layout and Setup Interface. (**A**) When the RedoxMetrics macro-set for FIJI is installed, a number of new macro commands as well as a set of action tools to test and optimize the analysis settings is created in the menu bar. 'S' invokes the setup interface. 'F' performs a flatfield correction on an open image. 'C' and 'M' perform a test segmentation for cellular regions ("Cell", CM-H2DCFDA channel) and mitochondrial regions ("Mito", TMRM channels), respectively on a single opened image using the analysis settings selected in the setup interface, returning an overlay of the segmented regions of interest (ROIs). '#' performs batch analysis on a folder of images using the settings specified in the setup interface (usually after verification on one or a few images). 'V' creates a verification hyperstack using the output data from the batch analysis. This hyperstack is a composite image of all raw images present in the folder and their respective regions of interest (drawn in a second channel). 'O' can be clicked to show or hide the overlay of the segmented region. (**B**) Setup interface. Here all analysis settings are selected, including general information such as the image type (extension), number of channels (wavelengths), and the well that was used for flatfield correction. Next there are settings specific to the image content type (Cell or Mito). In both cases, there are options (checkboxes) to include a background correction ("background") and local contrast enhancement ("contrast"). For cell segmentation, there is the option to define a Gaussian blur radius (sigma) for reducing noise. For mito segmentation there is the option to define the radius of a Laplacian operator for selective enhancement of the mitochondria. Subsequent segmentation is performed using an automatic (or fixed) thresholding method that can be defined per content type. When a fixed threshold is chosen, the upper threshold value can be provided manually. Finally, the analysis can be restricted to a selection of objects that falls within a minimum and max size. (**C**) An example of a segmentation result as run with the "C" (top) or "M" (bottom) command, displayed as the raw image in grey overlaid with the regions of interest in yellow. Please click here to view a larger version of this figure.

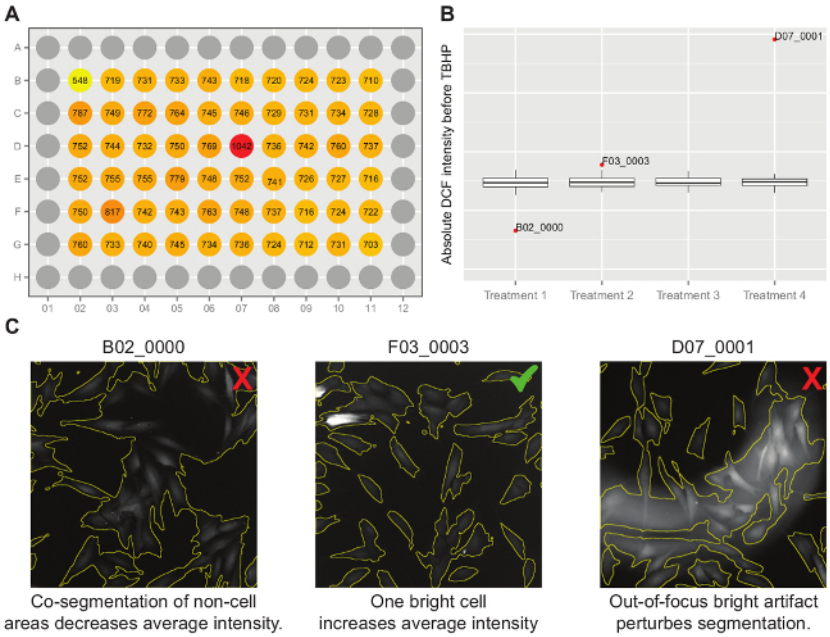

Figure 4: Illustrated Example of Intermediate Data Visualizations. (**A**) Multiwell plate visualization where wells B02 and D07 appear suspicious. (**B**) Boxplot representing the same data, with the outliers labeled with well name and image name. Together with F03_0003, images from B02 and D07 reappear as outliers. (**C**) Visual inspection of these images shows that B02_0000 and D07_0001 should be removed from further analysis because there are segmentation errors (illustrated by the red 'X'). F03_0003 should be kept because there is no apparent segmentation or technical error. (if no technical reason is found for the aberration, the data should not be removed). Please click here to view a larger version of this figure.

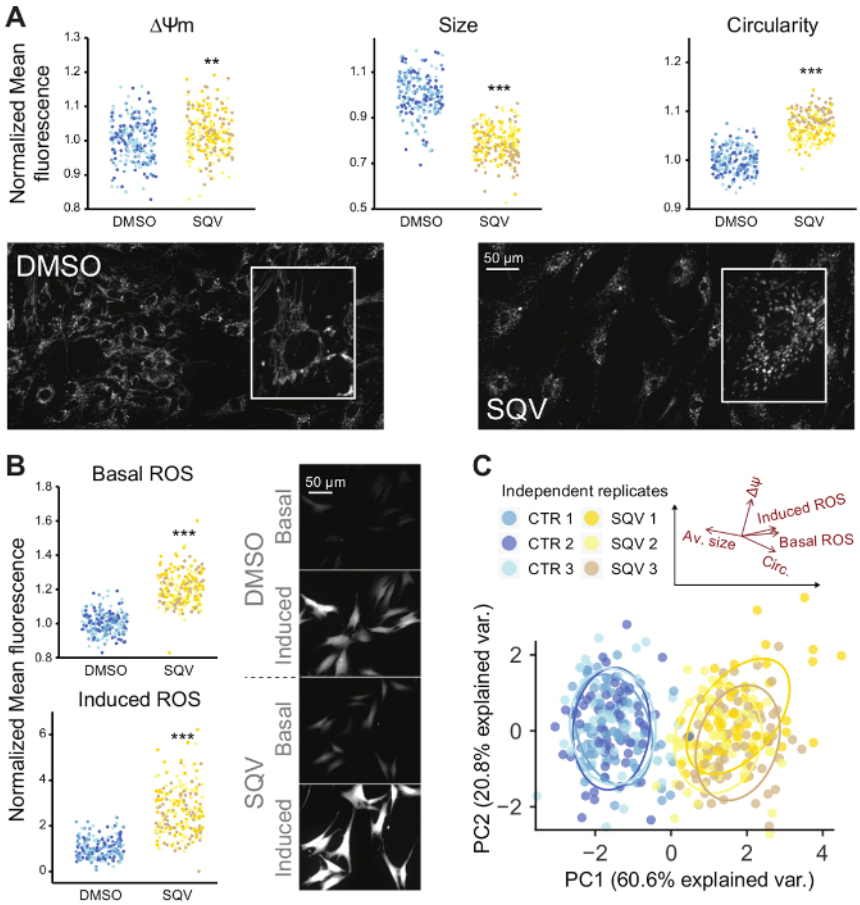

Figure 5: Effect of Saquinavir (SQV; 20 µM) on Primary Human Fibroblasts (control is DMSO). (**A**) Mitochondrial membrane potential ($\Delta\Psi_m$) and mitochondrial morphology (circularity and average size of individual mitochondria) as measured by TMRM (**B**) Increased Basal levels of intracellular ROS as measured by CM-H_2DCFDA and response towards induced ROS, measured as relative gain in intensity after addition of 20µM TBHP addition. (**C**) 2D scatterplot of the first 2 principal components (PCs) from a PCA analysis on the 5 variables described above (basal and induced ROS levels, average mitochondrial size, circularity, and $\Delta\Psi_m$). The black arrows represent the directions of the original 5 variables with respect to the principal components. (Independent replicates are plotted with a different color; All data is normalized with respect to the DMSO-control; * = p value <0.05; ** = p value <0.01; *** = p value <0.001; the range of the Y -axes has been adjusted to optimally display the differences; This figure was modified from reference[1], with permission of Springer) Please click here to view a larger version of this figure.

Problem	Potential reason	Possible solution
Too few cells in the wells during imaging	Too few cells seeded	Seed more cells 24 h before imaging
	Poor cell growth	Check culture conditions (medium, temperature stability, CO_2 control)
	Too violent washing steps	Avoid washing cells away, pipette gently
Too many cells in the wells during imaging	Too many cells seeded	Seed less cells 24 h before imaging
Weak signals or non-linear response of CM-H_2DCFDA fluorescence to stimulus	Used too low/high dye concentration	If using other than NHDF cells, optimal loading concentrations have to be determined empirically
	Dye-loading is insufficient	Add 0.02% w/v of the surfactant Pluronic-127 to the loading solution to increase uptake.
CM-H_2DCFDA signal visually increases during exposure time	Too high dye concentration	Reduce dye concentration
	Excitation intensity is too high	Reduce excitation intensity by using ND filters and/or reducing exposure time
CM-H_2DCFDA intensity decreases during acquisition of the well plate	CM-H_2DCFDA is leaking out of the cell.	Use 2 mM Probenicid (anion pump inhibitor). Add to the loading solution, as well as the imaging buffer to decrease leakage
There is no increase in CM-H_2DCFDA signal intensity after addition of TBHP	TBHP is not active	Use fresh TBHP
	CM-H_2DCFDA is leaking out of the cell.	Use Probenicid as described above.
(Some of the) acquired images appear out-of-focus, while focus seems ok when checked.	The plate is mounted tilted causing the focus to extend beyond the PFS offset	Check the mounting of the plate and the stage level, Reposition the plate
	The bottom of the plate contains dust or irregularities	Clean the bottom of the plate with an ethanol-wetted lens paper
Cells die during imaging	Excitation intensity is too high	Reduce excitation intensity or acquire fewer images per well.
	Wrong imaging-buffer composition	Remake imaging-buffer
There are out of focus fluorescent spots in the images	Detached cells are floating out of focus	Wash more gently during the loading protocol
One or more columns have an allover lower intensity than the other wells of the plate	One or more tips from the multichannel pipette were not firmly attached and therefore less reporter was added to these wells	Thoroughly check if all tips are filled perfectly whenever you use a multichannel pipette.
Focus drifts dramatically during image acquisition	The polystyrene bottom of the plate can react with immersion oil when using an oil lens	Use a dry lens, or use a multiwell plate with a glass bottom
TMRM signal intensity increases between imaging the first and last well	Reporter loading time was not long enough, TMRM is still equilibrating	Increase reporter loading time
CM-H_2DCFDA signal after TBHP treatment increases during acquisition of the well plate	The time between treatment with TBHP and the start of the second imaging round was not long enough, TBHP is still oxidizing CM-H_2DCFDA.	Increase incubation time between the treatment with TBHP and the second imaging round. (start with at least 3 min)
Flat field images are saturated	Antibody working solution is to concentrated	Use a lower concentration of antibody working solution
	Acquisition settings are not optimized (exposure time to high, ND-filter to low, …)	Optimize acquisition settings, signal has to be in dynamic range of the sensor
Flat field images are to dark	Antibody working solution is to diluted	Use a higher concentration of antibody working solution
	Acquisition settings are not optimized (exposure time to high, ND-filter to low, …)	Optimize acquisition settings, signal has to be in dynamic range of the sensor
Over/Undersegmentation artefacts	Threshold not set correctly	Adjust the threshold setting
	Size filters not adjusted properly	Adjust the min and max size criteria for image analysis
	Cell confluency is too high	The correct level of confluency is very important for reliable image analysis. For other cell types than NHDF, the optimal seeding density has to be determined empirically
The shiny application does not work	Wrong directory selected	Choose the correct directory on the input page.

	Missing files in directory	Make sure all necessary files (output from imagej macro and setup file) are present in the selected directory
	Missing packages	Normally the app checks for and installs all necessary packages, but when this fails, check manually for the following packages: devtools, ggbiplot, pacman, ggplot2, plyr, nparcomp, data.table, readxl, gplots, ggbiplot, shiny, shinyFiles, pbapply and shinyjs including all dependencies.

Table 1: Typical pitfalls and potential solutions.

Discussion

This paper describes a high-content microscopy method for the simultaneous quantification of intracellular ROS levels and mitochondrial morphofunction in NHDF. Its performance was demonstrated with a case study on SQV-treated NHDF. The results support earlier evidence from literature in which increased ROS levels or mitochondrial dysfunction have been observed after treatment with type 1 HIV protease inhibitors, albeit in separate experiments[19,20,21,22,23,24,25]. The important difference is that the described assay is able to measure these parameters simultaneously, in the same living cells, together with morphological data. The major advantage of this approach is its unambiguous determination of both factors together in space and time, which allows pinpointing causal relationships. A principal component analysis is performed which allows for generating a sensitive redox profile of specific perturbations. However, more advanced data mining techniques and (supervised) clustering algorithms can also be used on the extracted data to enable predictive redox profiling. This may be a valuable feature for diagnostic or prognostic classification tools in digital pathology, as well as in screening for therapeutic targets, *e.g.* once robust classification models are created, small molecule libraries can be screened to find therapeutic candidates to counteract oxidative stress, analogous to a recent screen for promising leads in therapy development for human mitochondrial disorders[26].

The assay was conceived for NHDF, but can be adapted to other adherent cell types. This requires optimization of the staining protocol and reporter dye concentrations. The amount of reporter dye has to be minimized since overloading can cause nonlinear effects due to quenching or even become cytotoxic[27]. Extension of the assay to suspension cells is less obvious due to difficulties with mounting and observing such cells in a physiological manner. They can be cytospun on a coverslip or cultured in serum-free media to induce adhesion, but both of these processes interfere with physiological conditions[28,29]. However, these limitations could be overcome using micropatterned cell culture supports that keep individual cells (adherent or non-adherent) trapped in small micro wells while maintaining their viability[30], or by the use of a thermo-reversible hydrogel to trap cells during imaging[31]. These methods have already been used for high-content screening of plasma membrane potential, or cellular oxygen in individual suspension cells[32,33] or the imaging of intracellular markers in the living, highly motile parasites[31]. Adaptations would also have to be made to the imaging modality, since morphological analysis of the mitochondrial network in these cells would require rapid 3D-acquisition capabilities such as spinning disk confocal or Bessel beam light sheet microscopy[34,35], as well as to the analysis pipeline, to include the Z-dimension while calculating morphological parameters.

The assay was optimized for 96-well plates, but it is obviously amenable to further upscaling, *e.g.* to 384-well plates. The major limiting factor is the plate acquisition time, *i.e.,* the time it takes to acquire images of all the wells. The fluorescent signals have to remain stable during this timeframe so as to be able to confidently compare measurements between individual wells. But, because the staining is transient and the process under investigation is dynamic, this poses a challenge. Therefore, the fluorescent signals were measured in a set of replicated experiments and this showed that both CM-H_2DCFDA and TMRM signals remain stable from 7 to at least 50 min after staining (coefficient of variation <2%). This gives a window of approximately 40 min. A 96-well plate typically takes around 10 min. Thus, an extrapolation to 384-well plates would keep the acquisition duration within the stable time slot. With an average of 50 cells per image (based on the use of a 20X objective and NHDF cells), this would result in data for approximately 30,000 cells per hour of screening, greatly adding to the statistical power of the assay. Another factor influencing fluorescent signal stability is the temperature. To avoid vacuolization of CM-H_2DCFDA (i.e. dye accumulation in intracellular vesicles), which would give rise to heterogeneous staining and non-linear effects, the incubation takes place at room temperature instead of 37 °C. Apart from stability, it is important to note that the exposure of living cells to fluorescence excitation light itself induces ROS production. This implies that the exposure conditions (exposure time and excitation light intensity) should be kept at an absolute minimum. It also means that all wells should only be exposed when the actual images are acquired. This rules out the use of software-enabled autofocusing methods and warrants the use of a hardware-based autofocus system.

An advantage of the described method is its generic character. Virtually any combination of spectrally compatible fluorescent reporters can be used. This was demonstrated by using the Calcein/MitoSOX combination to measure mitochondrial ROS per living cell[1,15]. Furthermore, the applications are not limited to the integrated ROS/mitochondrial measurement. The assay can also be extended with a *post hoc* immunostaining (after the second imaging round). Since the exact imaging locations are saved, redox analyses can be directly correlated with location proteomics in the same cells. This greatly increases the molecular readout, which is in stark contrast to other methods often used to assess redox biology, or fluorescence intensities in general. For instance, fluorimetry (microplate reader) is widely used because of its relatively low cost (basic setup available for as low as €4000) and shallow learning curve, but being a black box, it is more prone to confounding factors such as variations in cell density or background (auto-)fluorescence, *e.g.* of contaminating dust particles. Moreover, plate readers do not allow for the extraction of morphological parameters, they cannot measure single cells, and they are less sensitive and reliable to measure dynamic or transient signals[36,37]. Flow cytometry does have the capacity to measure single cells and has the advantage of speed. Indeed, a 384-well plate can be screened in as little as 12 min with high sensitivity for multiple markers[38]. This is much faster than what is possible with widefield microscopy. But, still no spatiotemporal information is provided (*i.e.* subcellular localization, morphological data and/or time dependent kinetics), nor does it allow revisiting the same cells during or after a treatment *(i.e., in fluxo)*. Furthermore, cells need to be in suspension, which makes flow cytometry less suited to studying the physiology of adherent cells. Major disadvantages of high-content microscopy as compared to the other methods are the need for large image data storage, intensive processing power and complex image analyses. The presented assay

standardizes the image acquisition process and streamlines the analysis so as to minimize this processing time, increase ease of use and therefore make the assay more accessible.

In conclusion, and specific to the use of CM-H_2DCFDA and TMRM, the described redox profiling method is robust, sensitive and reliable. Due to its multiparametric and quantitative nature, it is superior to other fluorescence-based methods. This way, it can help to elucidate the relationship between mitochondrial function and intracellular ROS signaling, which is crucial for better understanding a wide variety of pathologies in which redox homeostasis is perturbed. Furthermore, owing to its generic character, the assay allows applications well beyond its original scope.

Disclosures

The authors state that there are no competing financial interests or other conflicts of interest. The corresponding author also ensures that all authors have been asked to disclose any and all conflicts of interest.

Acknowledgements

This research was supported by the University of Antwerp (TTBOF/29267, TTBOF/30112), the Special Research Fund of Ghent University (project BOF/11267/09), NB-Photonics (Project code 01-MR0110) and the CSBR (Centers for Systems Biology Research) initiative from the Netherlands Organization for Scientific Research (NWO; No: CSBR09/013V). Parts of this manuscript have been adapted from another publication[1], with permission of Springer. The authors thank Geert Meesen for his help with the widefield microscope.

References

1. Sieprath, T., Corne, T. D. J., Willems, P. H. G. M., Koopman, W. J. H., & De Vos, W. H. Integrated High-Content Quantification of Intracellular ROS Levels and Mitochondrial Morphofunction. *AAEC.* **219** (Chapter 6), 149-177 (2016).
2. Marchi, S., *et al.* Mitochondria-ros crosstalk in the control of cell death and aging. *J Signal Transduct.* **2012** (article ID 329635), 1-17 (2012).
3. Korshunov, S. S., Skulachev, V. P., & Starkov, A. A. High protonic potential actuates a mechanism of production of reactive oxygen species in mitochondria. *FEBS lett.* **416** (1), 15-18 (1997).
4. Miwa, S., & Brand, M. D. Mitochondrial matrix reactive oxygen species production is very sensitive to mild uncoupling. *Biochem Soc Trans.* **31** (Pt 6), 1300-1301 (2003).
5. Verkaart, S., *et al.* Superoxide production is inversely related to complex I activity in inherited complex I deficiency. *BBA-Gen Subjects.* **1772** (3), 373-381 (2007).
6. Murphy, M. P. How mitochondria produce reactive oxygen species. *Biochem J.* **417** (pt 1), 1-13 (2009).
7. Lebiedzinska, M., *et al.* Oxidative stress-dependent p66Shc phosphorylation in skin fibroblasts of children with mitochondrial disorders. *BBA-Gen Subjects.* **1797** (6-7), 952-960 (2010).
8. Forkink, M., *et al.* Mitochondrial hyperpolarization during chronic complex I inhibition is sustained by low activity of complex II, III, IV and V. *BBA-Bioenergetics.* **1837** (8), 1247-1256 (2014).
9. Willems, P. H. G. M., Rossignol, R., Dieteren, C. E. J., Murphy, M. P., & Koopman, W. J. H. Redox Homeostasis and Mitochondrial Dynamics. *Cell Metab.* **22** (2), 207-218 (2015).
10. Koopman, W. J. H., *et al.* Human NADH:ubiquinone oxidoreductase deficiency: radical changes in mitochondrial morphology? *Am J Physiol Cell Physiol .* **293** (1), C22-C29 (2007).
11. Archer, S. L. Mitochondrial dynamics--mitochondrial fission and fusion in human diseases. *N Engl J Med.* **369** (23), 2236-2251 (2013).
12. Rambold, A. S., Kostelecky, B., Elia, N., & Lippincott-Schwartz, J. Tubular network formation protects mitochondria from autophagosomal degradation during nutrient starvation. *Proc Natl Acad Sci U S A.* **108** (25), 10190-10195 (2011).
13. Koopman, W. J. H., *et al.* Simultaneous quantification of oxidative stress and cell spreading using 5-(and-6)-chloromethyl-2 ",7 -"dichlorofluorescein. *Cytometry A.* **69A** (12), 1184-1192 (2006).
14. Iannetti, E. F., Smeitink, J. A. M., Beyrath, J., Willems, P. H. G. M., & Koopman, W. J. H. Multiplexed high-content analysis of mitochondrial morphofunction using live-cell microscopy. *Nat Protoc.* **11** (9), 1693-1710 (2016).
15. Sieprath, T., *et al.* Sustained accumulation of prelamin A and depletion of lamin A/C both cause oxidative stress and mitochondrial dysfunction but induce different cell fates. *Nucleus.* **6** (3), 236-246 (2015).
16. Zuiderveld, K. Contrast limited adaptive histogram equalization. *Graphics gems IV.*, 474-485 Academic Press Professional, Inc.: (1994).
17. Chang, W., Cheng, J., Allaire, J. J., Xie, Y., & McPherson, J. *shiny: Web Application Framework for R. R package version 0.14.2.* at <https:// CRAN.R-project.org/package=shiny >(2017).
18. Konietschke, F., Placzek, M., Schaarschmidt, F., & Hothorn, L. A. nparcomp: An R Software Package for Nonparametric Multiple Comparisons and Simultaneous Confidence Intervals. *J Stat Softw.* **64** (9), 1-17,doi:10.18637/jss.v064.i09 (2015).
19. Estaquier, J., *et al.* Effects of antiretroviral drugs on human immunodeficiency virus type 1-induced CD4(+) T-cell death. *J Virol .* **76** (12), 5966-5973 (2002).
20. Matarrese, P., *et al.* Mitochondrial membrane hyperpolarization hijacks activated T lymphocytes toward the apoptotic-prone phenotype: homeostatic mechanisms of HIV protease inhibitors. *J Immunol.* **170** (12), 6006-6015 (2003).
21. Roumier, T., *et al.* HIV-1 protease inhibitors and cytomegalovirus vMIA induce mitochondrial fragmentation without triggering apoptosis. *Cell Death Differ.* **13** (2), 348-351 (2006).
22. Chandra, S., Mondal, D., & Agrawal, K. C. HIV-1 protease inhibitor induced oxidative stress suppresses glucose stimulated insulin release: protection with thymoquinone. *Exp Biol Med (Maywood) .* **234** (4), 442-453 (2009).
23. Touzet, O., & Philips, A. Resveratrol protects against protease inhibitor-induced reactive oxygen species production, reticulum stress and lipid raft perturbation. *AIDS.* **24** (10), 1437-1447 (2010).
24. Bociąga-Jasik, M., *et al.* Metabolic effects of the HIV protease inhibitor--saquinavir in differentiating human preadipocytes. *Pharmacol Rep .* **65** (4), 937-950 (2013).

25. Xiang, T., Du, L., Pham, P., Zhu, B., & Jiang, S. Nelfinavir, an HIV protease inhibitor, induces apoptosis and cell cycle arrest in human cervical cancer cells via the ROS-dependent mitochondrial pathway. *Cancer Lett.* **364** (1), 79-88 (2015).
26. Blanchet, L., Smeitink, J. A. M., *et al.* Quantifying small molecule phenotypic effects using mitochondrial morpho-functional fingerprinting and machine learning. *Sci. Rep.* **5**, 8035 (2015).
27. Invitrogen. *Reactive Oxygen Species (ROS) Detection Reagents.* Accessed 22 Apr (2015).
28. Koh, C. M. Preparation of cells for microscopy using cytospin. *Methods Enzymol.* **533**, 235-240 (2013).
29. Mihara, K., Nakayama, T., & Saitoh, H. A Convenient Technique to Fix Suspension Cells on a Coverslip for Microscopy. *Curr Protoc Cell Biol* ***68***., 4.30.1-10 (2015).
30. Deutsch, M., Deutsch, A., *et al.* A novel miniature cell retainer for correlative high-content analysis of individual untethered non-adherent cells. *Lab Chip.* **6** (8), 995-6 (2006).
31. Price, H. P., MacLean, L., Marrison, J., O'Toole, P. J., & Smith, D. F. Validation of a new method for immobilising kinetoplastid parasites for live cell imaging. *Mol Biochem Parasitol.* **169** (1), 66-69 (2010).
32. Sabati, T., Galmidi, B.-S., Korngreen, A., Zurgil, N., & Deutsch, M. Real-time monitoring of changes in plasma membrane potential via imaging of fluorescence resonance energy transfer at individual cell resolution in suspension. *JBO.* **18** (12), 126010 (2013).
33. Fercher, A., O'Riordan, T. C., Zhdanov, A. V., Dmitriev, R. I., & Papkovsky, D. B. Imaging of cellular oxygen and analysis of metabolic responses of mammalian cells. *Meth Mol Biol.* **591** (Chapter 16), 257-273 (2010).
34. Graf, R., Rietdorf, J., & Zimmermann, T. Live cell spinning disk microscopy. *Adv. Biochem. Eng. Biotechnol.* **95** (Chapter 3), 57-75 (2005).
35. Gao, L., Shao, L., Chen, B.-C., & Betzig, E. 3D live fluorescence imaging of cellular dynamics using Bessel beam plane illumination microscopy. *Nat. Protoc.* **9** (5), 1083-1101 (2014).
36. Meijer, M., Hendriks, H. S., Heusinkveld, H. J., Langeveld, W. T., & Westerink, R. H. S. Comparison of plate reader-based methods with fluorescence microscopy for measurements of intracellular calcium levels for the assessment of in vitro neurotoxicity. *Neurotoxicology.* **45**, 31-37 (2014).
37. Bushway, P. J., Mercola, M., & Price, J. H. A comparative analysis of standard microtiter plate reading versus imaging in cellular assays. *Assay and drug development technologies.* **6** (4), 557-567 (2008).
38. Black, C. B., Duensing, T. D., Trinkle, L. S., & Dunlay, R. T. Cell-Based Screening Using High-Throughput Flow Cytometry. *Assay Drug Dev Technol.* **9** (1), 13-20 (2011).

